

Compensation Structures for Convex Corner Micromachining in Silicon

B. PUERS and W. SANSEN

Katholieke Universiteit Leuven, Departement Elektrotechniek, E.S.A.T., Kardinaal Mercierlaan 94, B-3030 Heverlee (Belgium)

Abstract

In order to gain precise information on the convex corner undercutting when using anisotropic etchants for silicon, a test mask has been elaborated, incorporating structures with orientations different from those of the wafer flats. The aim is to determine the behaviour of the etchants in terms of crystal orientation. These masks allow an insight to be gained into crystal-dependent etch rates, focusing in detail on the $\langle 120 \rangle$ and $\langle 130 \rangle$ directions. A second set of masks has been developed with an integrated edge compensation, using the etch depth as a parameter. This results in a novel compensation technique for preventing convex corner undercutting. Two types of etchant compositions are examined: an aqueous solution of KOH, and the same solution in combination with isopropyl alcohol (IPA); the first etchant has distinct advantages when precise convex corners are required.

Introduction

When etching rectangular convex corners in silicon using anisotropic etchants such as EDP or KOH [1-4], deformation of the edges always occurs due to underetching. This is an unwanted effect in micromachining silicon, e.g., in the fabrication of mechanical sensors for measuring acceleration, where perfect 90° convex corners are mandatory for good device prediction and specification. Therefore, an investigation was carried out in order to understand better the behaviour of the chemical etchants with respect to crystal orientation. The undercutting is a function of etch time, so it is also directly related to the desired etch depth. Depending on the type of etchant composition, a different structure is achieved. Figures 1 and 2 show typical examples of this undercutting phenomenon, for KOH etchants containing isopropyl alcohol (IPA), and for an IPA-free KOH solution respectively. In order to be able to propose a valuable compensation structure, several underetched rectangular corners were examined.

Based on these measurements, some compensation masks were elaborated.

Determining Preferential Etch Planes

Before making any test mask or test structure, the convex corner attack was studied on etched masses for accelerometer devices [5], in order to obtain information about possible preferential etch planes in silicon. All experiments were carried out on (100)-oriented n-type silicon wafers, double-side polished with a resistivity of $10 \Omega \text{ cm}$ and of $380 \mu\text{m}$ thickness. A nitride mask was used, and etching was carried out at 80°C in a water-potassium hydroxide solution.

Etching with IPA

Figure 3 shows the definition of the angles measured for determining the etch planes. The following results are obtained:

$$a = 131^\circ \pm 5^\circ \quad (n = 16)$$

$$b = 140^\circ \pm 4^\circ \quad (n = 16)$$

$$c = 20^\circ \pm 2^\circ \quad (n = 32)$$

These directions can best be matched with the $\langle 120 \rangle$ directions, for which a should measure 127° and $b = 143^\circ$. In order to determine the corresponding plane, a cross-section is made through the line AA' . One obtains:

$$e = 46^\circ \pm 1^\circ \quad (n = 6)$$

Looking for the most tightly packed lattice planes that cross the wafer surface at the $\langle 120 \rangle$ directions yields the (211) and the (212) planes. This corresponds with the work of Wu and Ko [6]. For these planes, the corners e are 65° and 48° respectively. Therefore, we conclude that the bevelling planes have to be (212) planes. d is a measure for the undercutting, which is dependent on the etch depth (ed). The relative undercutting d/ed is typically 1 to 1.1.

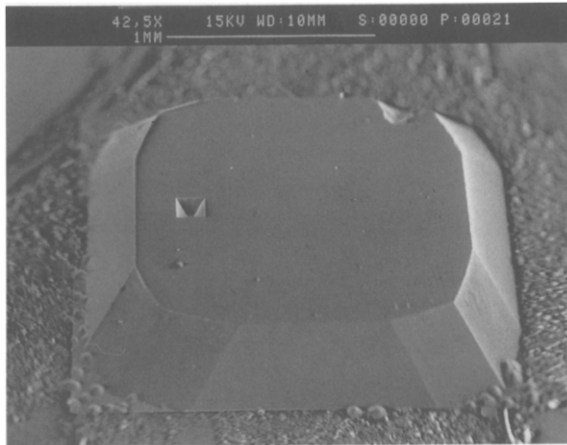


Fig. 1. Typical example of a rectangular mass, etched in a KOH solution with isopropyl alcohol (IPA). Note the rounded corners of the (accelerometer) mass.

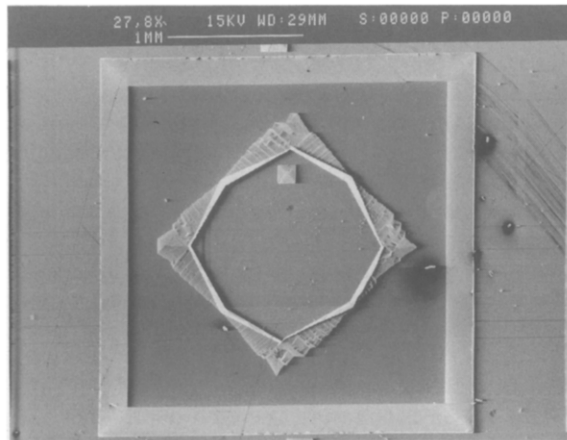


Fig. 2. SEM picture of the same rectangular mass as in Fig. 1, but etched in a pure KOH-water solution. The underetching is much more pronounced.

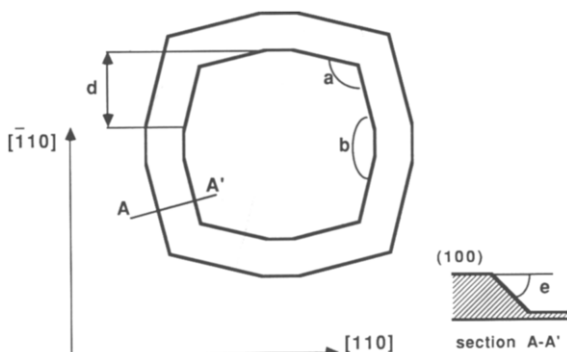


Fig. 3. Top view of an etched rectangular mass, with the definition of the measured angles. AA' is a cross-section perpendicular to the top contour line.

Etching without IPA

First, it is important to notice that the undercutting is much more severe without IPA in the solution. Also, several beveling planes intersect (see Fig. 2), which makes it virtually impossible to determine them exactly. However, an estimate for the direction can be measured from the intersection line. Figure 3 for this case yields:

$$a = 145^\circ \pm 1^\circ \quad (n = 8)$$

$$b = 125^\circ \pm 1^\circ \quad (n = 8)$$

which corresponds with $a = 143^\circ$ and $b = 127^\circ$ for the intersection lines for the $\langle 130 \rangle$ directions. We thus conclude that for this composition, the $\langle 130 \rangle$ direction is predominant in the underetched structure. This is in contrast with the work of Wu and Ko [6], who find the same beveling planes ($\langle 120 \rangle$ directions) for all etchants.

The undercutting ratio d/ed is much larger here, and is about 3.5. This means that any compensation structure for use with KOH only will have to be three times as large as when using KOH-IPA.

Tests and Measurements on Dedicated Test Masks

Figures 4 and 5 show two different test masks in order to determine the orientation dependence of the etchants with respect to several crystal orientations and the $\langle 120 \rangle$ and $\langle 130 \rangle$ directions in particular. The mask of Fig. 5 contains a quadrangle composed of both these directions.

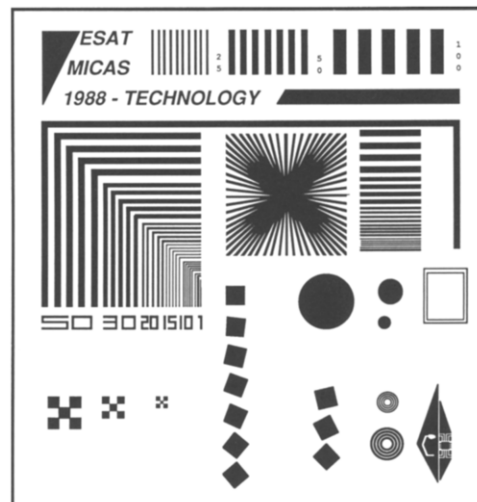


Fig. 4. Test mask for determining general etch behaviour of the selective etchants. Circles, a star-like configuration and rotated rectangles allow orientation-dependent etch rates to be measured.

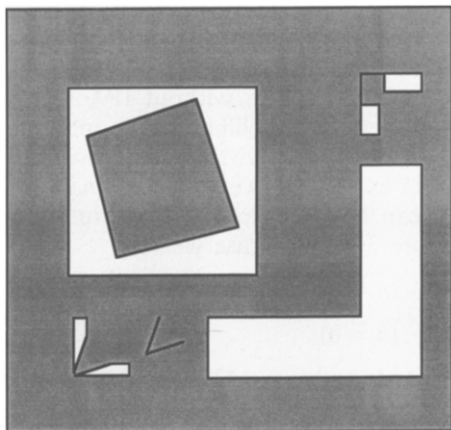


Fig. 5. Test mask to determine $\langle 120 \rangle$ and $\langle 130 \rangle$ preferential etch mechanisms.

From this experiment, the underetch rate perpendicular to these directions can be derived. Figure 6 is a plot of the results. It shows that the rate is typically $0.40 \mu\text{m}$ per micron etched in depth. From these results, the lateral etch or undercutting can also be derived (d in Fig. 3), yielding about $1.2 \mu\text{m}/\mu\text{m}$. From the previous experiments, this calculated e/ed is about 10% larger than measured on the former accelerometer mesas. This may be due to the fact that for the undercutting, other planes have to be attacked first before the (212) planes can be set free.

For any orientations other than $\langle 100 \rangle$ one can notice that all directions are attacked more or less in the same way, and that the bevelling planes remained unaffected. The underetching is a smooth function of the orientation, with no preferential attack of the slope. This is only affected if convex corners are present, where rounding off is started by the etching of $\langle 120 \rangle$ -oriented planes. It seems that the addition of IPA allows etching of

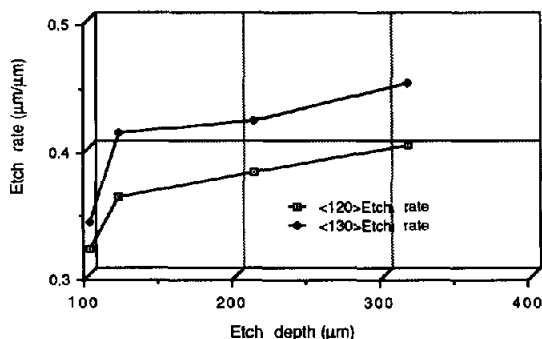


Fig. 6. Graph of the underetch rate of the $\langle 120 \rangle$ and $\langle 130 \rangle$ orientations for a KOH-IPA solution as a function of etch depth.

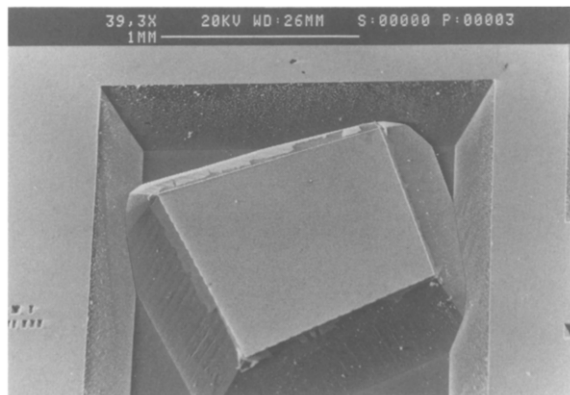


Fig. 7. SEM picture of a $300 \mu\text{m}$ deep etched structure along the $\langle 120 \rangle$ (top) and $\langle 130 \rangle$ (bottom) directions. Note the smooth surface of the slope, and the perfect parallel underetching to the original mask (see Fig 5). Note also the right angles.

any geometry in the silicon, with the vertical slope determined by the intersection of $\langle 120 \rangle$ -oriented planes and the $\{111\}$ planes, but always leaving a smooth surface. The SEM picture in Fig. 7 clearly illustrates this. Perfect convex corners can thus be achieved by orienting the structure according to the $\langle 120 \rangle$ orientations on the wafer.

Using an alcohol-free KOH solution results in a deviation of the $\langle 120 \rangle$ directions, leaving a quadrangle determined by $\langle 130 \rangle$ directions only. The etch behaviour is much more violent when compared with IPA-containing solutions, but distinct planes are set free. Figure 8 shows the relative etch rate perpendicular to the $\langle 130 \rangle$ orientation as a function of the etch depth. The rate is constant and independent of the etch depth, and equals $1.7 \mu\text{m}/\mu\text{m}$. This is in sharp contrast with Fig. 6, and is another indication for the more complex etching behaviour of KOH when IPA is added.

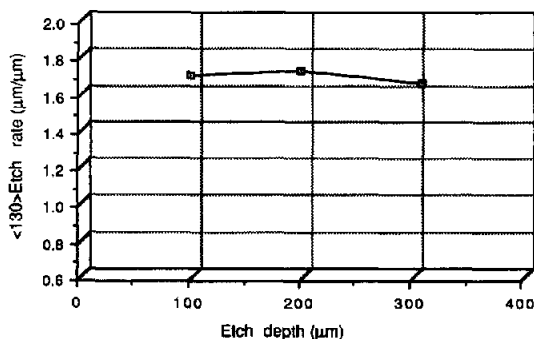


Fig. 8. Graph of the underetch rate of the $\langle 130 \rangle$ orientations for a KOH solution as a function of etch depth.

Derived Compensation Structures

Based on the knowledge that certain planes are etched parallel with the masking outline, some compensation patterns were elaborated for the formation of convex corners in silicon. A set of masks was developed with an integrated edge compensation, using the etch depth as a parameter, and all oriented to the $\langle 120 \rangle$ or $\langle 130 \rangle$ directions. Figure 9 shows three different compensation structures, which are based on the idea of having these directions as preferential etch planes. The most straightforward structure is composed of a triangle, composed by the $\langle 120 \rangle$ directions. During etching, this triangle will be etched away, leaving a 90° corner. The two other structures, a flattened triangle and a rectangular compensation pattern, are shortened-down versions of the same structure in order to save space. In fact, by creating new 90° convex corners, so that these will be etched away at the same time as the other planes are 'consumed', extensive space can be saved. The smaller rectangular pattern allows the same compensation effect to be achieved as the larger triangle. Figure 10 illustrates the mechanism of undercutting occurring at the rectangular compensation structure: four different $\langle 120 \rangle$ orientations attack the convex corners of the compensation rectangle until it is entirely 'consumed' to leave the desired 90° corner.

In the discussion, the term 'relative dimension' means the equivalent dimension of a triangle to obtain the same effect. Theoretically, all relative dimensions are the same.

A mask set containing 72 different edge patterns was designed in order to obtain information on the undercutting for three different etch depths (100, 200 and 300 μm), two etchant compositions,

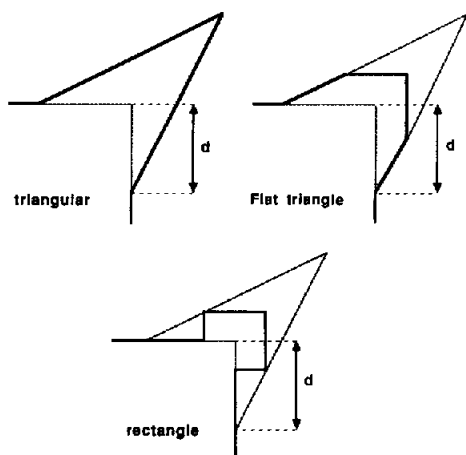


Fig. 9. Three different compensation techniques resulting in the same effect. d is the relative dimension.

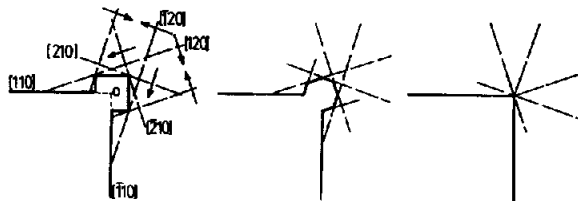


Fig. 10. Underetching procedure illustrating the compensation principle.

three compensation structures and four different undercutting ratios (e/ed). From this experiment, the following design recommendations for the compensation structures could be derived.

KOH + IPA Solution

The experiments have led to the optimization of the compensation pattern dimensions if a desired etch depth (ed) is given. All compensation structures are oriented according to the $\langle 120 \rangle$ orientation ($\langle 130 \rangle$ also works, but requires more space, and is therefore omitted). The relative dimensions for all the structures are respectively:

triangular:

$$\text{relative dimensions} = -1.7 + 1.16ed (\mu\text{m})$$

flat triangle:

$$\text{relative dimensions} = -5.3 + 1.24ed (\mu\text{m})$$

rectangular:

$$\text{relative dimensions} = -10 + 1.33ed (\mu\text{m})$$

Figure 11 summarizes the results. It shows that for a given etch depth, the optimal rectangular compensation technique requires a slightly larger relative dimension. However, since the absolute dimensions of the rectangular pattern are three times smaller, it remains the best-suited candidate for convex corner optimization.

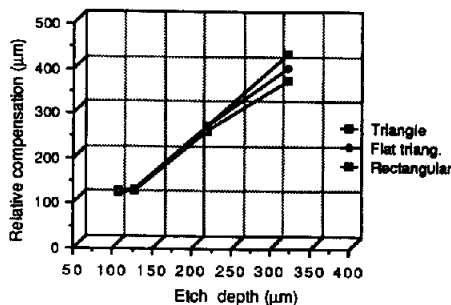


Fig. 11. Relative dimensions for the different compensation techniques to obtain a perfect right angle at the top of the mesa with a KOH-IPA solution.

KOH Solution

Based on the same techniques as above, the same kind of compensation approach can be elaborated for the use of KOH solution without IPA. The compensation structures will, however, be much larger, since the underetching itself is larger. Also, $\langle 130 \rangle$ -oriented compensation structures have to be adopted, which also requires more space. The experiments revealed the following optimal dimensions for the compensation structures:

triangular:

$$\text{relative dimensions} = 1.2 + 3.12ed (\mu\text{m})$$

flat triangle:

$$\text{relative dimensions} = 3.5 + 3.42ed (\mu\text{m})$$

rectangular:

$$\text{relative dimensions} = 5.7 + 3.72ed (\mu\text{m})$$

Figure 12 illustrates the definition of the relative dimension (d) for these formulae.

However, when etching in a KOH-water solution, a $\langle 110 \rangle$ compensation technique is possible, relying on the etching of these perpendicular planes [7]. Figure 12 illustrates the layout of such a compensation pattern, which is oriented along the $\langle 110 \rangle$ directions (45°). The bordering planes will be etched parallelly to one another, until the entire strip is consumed, setting free a perfect convex corner from top to bottom. Since they etch at the same etch rate as the (100) plane, the compensation geometry dimensions can be predicted quite obviously as:

$$-45^\circ \text{ compensation: } c = \sqrt{2}ed (\mu\text{m})$$

Care must be taken not to allow $\langle 130 \rangle$ directions to attack the protruding convex corners and underetch the compensation structure too early. Therefore, its length should be at least four times ed . Figure 13 illustrates this compensation technique in its almost final stage, revealing only a small portion of the original structure, bounded

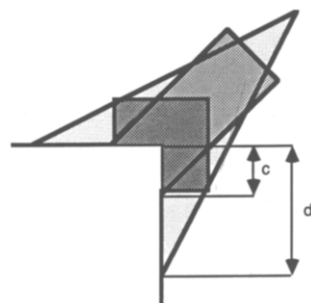


Fig. 12. Size comparison of the different compensation structures for use with KOH only. $\langle 130 \rangle$ orientation.

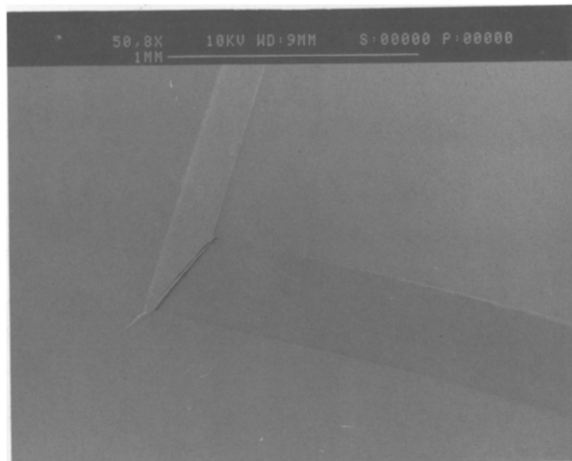


Fig. 13. SEM picture revealing the perfect 90° convex corner obtained with the $\langle 110 \rangle$ compensation in KOH-water solution.

by $\{010\}$ planes. Evidently, this is the most elegant compensation technique, providing enough space is available.

Conclusions

A non-compensated, underetched structure was measured in order to determine the best-suited compensation techniques for convex corner realization. This resulted in a set of differently shaped structures at the original 90° convex corner. Several geometries were elaborated, using $\langle 120 \rangle$, $\langle 130 \rangle$ and $\langle 110 \rangle$ directions in the compensation mask.

When using IPA-saturated KOH solutions, the $\langle 120 \rangle$ -based compensation is the only possible one for optimal convex 90° corner realization at the top of the wafer. Optimal results were obtained with a square-shaped compensation structure, in cases where minimal dimensions are important (e.g., narrow V-grooves). For a $1500 \times 1500 \mu\text{m}^2$ surface and an etch depth of $350 \mu\text{m}$, the compensation requires only an increase of 4% in surface of the original, non-compensated mask.

Isopropyl alcohol acts as an etchant 'softener' for all non- $\langle 100 \rangle$ directions: no planes are violently attacked, and large structures are conformally underetched with respect to the mask. Any convex corner is preferentially attacked by $\langle 120 \rangle$ -oriented planes.

Without IPA, KOH-based etchants can be compensated for underetching by $\langle 130 \rangle$ -oriented structures, which are typically three times larger (nine times for the surface) than the above compensation structures. An excellent alternative to this, but not

in terms of required space, is the $\langle 110 \rangle$ -oriented compensation, yielding perfect rectangular pyramidal mesas for micromachining masses of accelerometers or ring-shaped pressure sensors.

References

- 1 K. Bean, Anisotropic etching of silicon, *IEEE Trans. Electron Devices*, ED-25 (1978) 1185–1193.
- 2 E. Bassous, Fabrication of novel three-dimensional microstructures by anisotropic etching of (100) and (110) silicon, *IEEE Trans. Electron Devices*, ED-25 (1978) 1178–1185.
- 3 L. Csepregi, Micromechanics: a silicon microfabrication technology, *Microelectron. Eng.*, 3 (1985) 221–234.
- 4 H. Seidel and C. Csepregi, Three-dimensional structuring of silicon for sensor applications, *Sensors and Actuators*, 4 (1983) 445–463.
- 5 B. Puers, L. Reynaert, W. Snoeys and W. Sansen, A new uniaxial accelerometer in silicon based on the piezjunction effect, *IEEE Trans. Electron Devices*, ED-35 (1988) 764–770.
- 6 X. Wu and W. Ko, A study on compensating undercutting in anisotropic etching of silicon, *4th Int. Conf. Solid-State Sensors and Actuators (Transducers '87)*, Tokyo, Japan, June 2–5, 1987, pp. 126–129.
- 7 R. Buser and N. de Rooij, Monolithisches Kraftsensordfeld, *VDI Berichte Nr. 667, Sensoren, Technologien und Anwendung*, 1988, pp. 115–118.